

Sub-ms, nondestructive, time-resolved quantum-state readout of a single, trapped neutral atom

Margaret E. Shea* and Paul M. Baker

Department of Physics, Duke University, Durham, North Carolina 27708, USA

James A. Joseph and Jungsang Kim

Department of Electrical Engineering, Duke University, Durham, North Carolina 27708, USA

Daniel J. Gauthier

Department of Physics, The Ohio State University, Columbus, Ohio 43210 USA

(Dated: April 12, 2022)

We achieve fast, nondestructive quantum-state readout via fluorescence detection of a single ^{87}Rb atom in the $5S_{1/2}$ ($F = 2$) ground state held in an optical dipole trap. The atom is driven by linearly-polarized readout laser beams, making the scheme insensitive to the distribution of atomic population in the magnetic sub-levels. We demonstrate a readout fidelity of $97.6 \pm 0.2\%$ in a readout time of $160 \pm 20 \mu\text{s}$ with the atom retained in $> 97\%$ of the trials, representing a substantial advance over other magnetic-state-insensitive techniques. We demonstrate that the $F = 2$ state is partially protected from optical pumping by a fortuitous distribution of the dipole matrix elements for the various transitions and the AC-Stark shifts from the optical trap. Our results are likely to find wide application in neutral-atom quantum computing and simulation.

Optically-trapped neutral-atom qubits have emerged as a promising platform for quantum computing, quantum simulation [1–7], and the study of fundamental light-atom interactions [8, 9]. Most experiments require reading out the atom’s internal quantum state to determine the outcome of a given protocol, such as in quantum computation. It is desirable to perform the measurement with high fidelity in a short readout time without losing the atom from the trap so that the experiment can be repeated rapidly. This quantum-state readout requires balancing conflicting physical effects, such as heating from the fluorescent photons during readout and optical pumping of the atom to another state.

In this Letter, we use linearly-polarized light to discriminate between the two hyperfine ground states of a single ^{87}Rb atom via state-dependent fluorescence while it is held in an optical dipole trap (ODT). We use a single high-numerical-aperture lens to both create the optical trap and collect the atomic fluorescence. Under optimized conditions, we achieve a discrimination fidelity of $> 97\%$ in a measurement time of $160 \mu\text{s}$, which can be used as a state-readout of a qubit register. This is the fastest quantum-state readout yet reported for a single trapped neutral atom. In addition, by time-tagging the incoming photons and using a model of the readout protocol [10, 11], we determine the decay rate of the fluorescent light and identify atom heating as a primary factor limiting the system performance. Furthermore, we develop a rate-equation model for the fluorescence process [12], which reveals that the AC-Stark shifts help maximize the measurement fidelity.

In our experiments, quantum-state readout requires

measuring whether the ^{87}Rb atom is in the $F = 1$ or $F = 2$ hyperfine levels of the $5S_{1/2}$ ground state. These levels are shown in the inset of Fig. 1 and are labeled G_1 and G_2 , respectively (splitting $\Delta_G = 2\pi(6.8 \text{ GHz})$). Quantum-state readout is achieved via fluorescence detection using π -polarized light that is nearly resonant with the $5S_{1/2}(F = 2) \rightarrow 5P_{3/2}(F' = 3)$ transition ($G_2 \rightarrow E$) [13]. An atom in the $F = 2$ ground state scatters photons when illuminated by the readout beam and appears bright during the measurement time (the ‘bright state’), while atoms in the $F = 1$ ground state essentially do not fluoresce (the ‘dark state’) due to the large detuning Δ_G . The measurement decision as to whether the atom is bright or dark is based on recording a threshold number of photons n_{thresh} [14]. This readout scheme does not require optically pumping the atom into a particular magnetic sub-level before the measurement.

Previous studies have used fluorescence detection methods for nondestructive quantum-state readout of single atoms and arrays of trapped neutral atoms using circularly-polarized readout light [15–17], which requires pumping the atom into the $m_F = \pm F$ magnetic sub-level. The optical pumping process is hampered by the AC-Stark shifts caused by the ODT and requires a pumping time of the order of a few ms or turning off the ODT. Another study used linearly-polarized readout light [18], but did not focus on minimizing the measurement time.

Our experimental setup is shown in Fig. 1. A single ^{87}Rb atom is confined in an 1.28-mK -deep ODT created by a linearly-polarized, 852-nm -wavelength, 40-mW -maximum-power beam focused to an estimated $3\text{-}\mu\text{m}$ -waist ($1/e$ intensity diameter) by an off-the-shelf, $\text{NA}=0.54$ asphere mounted in the vacuum chamber. The atom is loaded into the ODT from a magneto-optical trap (MOT). Once loaded, the presence of the atom is verified using an atom detection sequence that cools

* corresponding author: margaret.shea@alumni.duke.edu

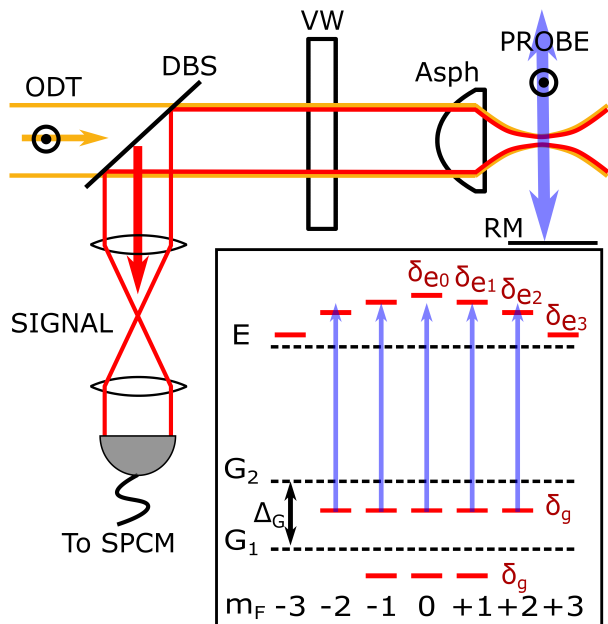


FIG. 1. The ODT light passes through the vacuum window (VW) and is focused by an asphere (Asph) to form the trap. The probe light is retroreflected by a mirror (RM) to produce counter-propagating beams. The signal is separated from the ODT light by a dichroic beamsplitter (DBS) before being directed to the SPCM. Inset: The atom is probed by the π -polarized probe light on the $G_2 \rightarrow E$ transition. The energy levels, hyperfine splittings (Δ) and AC-Stark shifts (δ) are defined in the text.

the atom during detection similar to that reported in [12, 19]. The quantum state of the atom is readout using counter-propagating laser beams linearly polarized along the same axis as the ODT beam, which is taken as the quantization axis. No external magnetic field is applied, greatly simplifying the experimental setup and required alignment. In the collection path, the atomic fluorescence is focused to an intermediate plane where a spatial filter reduces background scatter. The atomic fluorescence is coupled into a multimode fiber that directs it to a single photon counting module (SPCM) avalanche photodiode from Perkin-Elmer (part number AQR14+) with a dark count rate of 150 Hz. The multimode fiber acts as a secondary spatial filter to further reduce background counts.

The π -polarized ODT light shifts the magnetic sublevels of the atom due to the AC-Stark effect [19, 20], as shown in the inset of Fig. 1. The ground state magnetic sublevels uniformly shift $\delta_g = -27$ MHz, creating the trapping potential. The effect lifts the degeneracy of the $F' = 3$ (E) excited state with shifts of $\delta_{e0} = 21$ MHz, $\delta_{e1} = 19$ MHz, $\delta_{e2} = 13$ MHz, and $\delta_{e3} = 3$ MHz, yielding different resonance frequencies for each $\Delta m_F = 0$ transition probed by the linearly-polarized readout light. This causes a broadening of the atom's natural linewidth for π -polarized readout light tuned to the $F = 2 \rightarrow F' = 3$

transition [19]. We observe a broadened linewidth of ~ 13 MHz and find that the atomic fluorescence is maximized when the readout-beam frequency is detuned $+46$ MHz from the untrapped atom's resonance [12] (to the high-frequency side of the resonance), a frequency weighted towards the $m_F = 0$ transition frequency. This observation is consistent with the fact that the $m_f = 0$ transition has the largest Clebsch-Gordan coefficient and the population tends to accrue in the $m_F = 0$ state [12].

To determine the fidelity of the quantum-state readout protocol, the atom is first prepared into either the bright state ($F = 2$) by pumping the atom for $100 \mu\text{s}$ using the MOT repump beams, or the dark state ($F = 1$) by pumping the atom for 5 ms using the MOT cooling beams. The atom's state is measured using a single $200\text{-}\mu\text{s}$ -long readout pulse. If more than n_{thresh} photons are detected during the readout time, the atom is declared to be in the bright state ($F = 2$). If fewer than n_{thresh} photons are detected, the atom is declared to be in the dark state ($F = 1$). Once the readout is complete, another atom detection sequence is performed to verify that the atom remains in the trap and that the readout is nondestructive.

The readout fidelity is determined using the relation $\mathcal{F}_{n_{\text{thresh}}} = (\epsilon_B + \epsilon_D)/2$, where ϵ_B is the bright-state error, ϵ_D is the dark-state error, and n_{thresh} is the number of photons needed to classify the atom as bright or dark. By time-tagging the photon detection time relative to the start of the readout pulse, we can reconstruct the state readout fidelity during each $1 \mu\text{s}$ interval of the $200\text{-}\mu\text{s}$ -long readout time and for any photon number threshold, a measurement not previously reported for neutral atoms.

We find that $\mathcal{F}_{n_{\text{thresh}}}$ is optimized when the readout-beam frequency is $\nu_{23} + 40$ MHz, which is different from the frequency that maximizes the total fluorescence ($\nu_{23} + 46$ MHz). As seen in Fig. 2, the fidelity obtained using $n_{\text{thresh}} = 1$, denoted by \mathcal{F}_1 , has a maximum value of $95.0 \pm 0.3\%$ at a measurement time of $84 \pm 6 \mu\text{s}$. For thresholding on two photons ($n_{\text{thresh}} = 2$), denoted by \mathcal{F}_2 , a maximum fidelity of $97.6 \pm 0.2\%$ is obtained for a measurement time of $160 \pm 20 \mu\text{s}$. We find that using more than two photons to classify the atom as bright or dark does not improve the fidelity, in agreement with [15].

These curves represent several experimental runs totaling 3,583 experiments in which the atom is prepared in the bright state and 3,550 experiments in which the atom was prepared in the dark state. The data presented in Fig. 2 is post-selected for those events where an atom is retained in the trap. On average, the atom is retained in the trap after readout in $97.1 \pm 0.1\%$ of the experiments. This retention number is not corrected for background-induced losses.

Examining the photon arrival times shows that the atom's scattering rate decreases during the measurement. One possible cause of this loss is off-resonant pumping (ORP) causing the atom to drop into the $F = 1$ ground

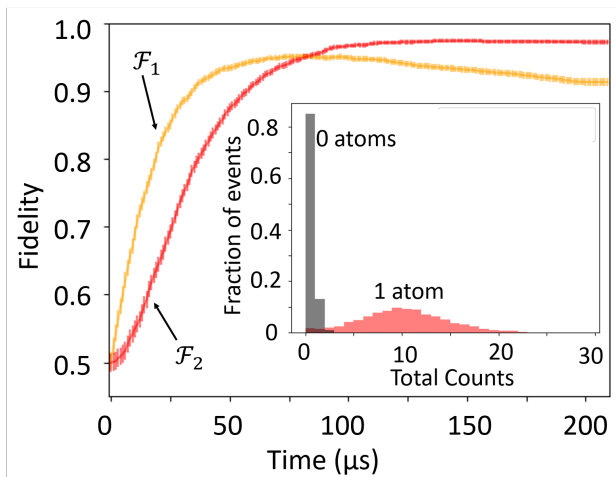


FIG. 2. \mathcal{F}_1 (yellow) and \mathcal{F}_2 (red) are determined for each μs during the 200 μs -long probe pulse. The inset shows the histograms of events used to generate the fidelity curves.

state [10, 16]. Naively, one would expect off-resonant pumping to be largest for frequencies tuned below the shifted resonance because such frequencies are closer to the $F' = 2$ excited state through which ORP occurs [21]. To test this, we prepare the atom in the bright state and perform state readout at three different probe frequencies. One readout is performed with the probe frequency set to +46 MHz shifted from the untrapped atomic resonance, the frequency at which the atomic fluorescence peaks. Another data set is taken at +40 MHz of the untrapped atomic resonance, where we find the peak readout fidelity, and a third at +52 MHz of the untrapped resonance.

To quantify the scattering rate loss, we turn to a model developed by the ion trap community to describe fluorescence detection [10, 11]. The model contains the scattering rate detected from an atom in the bright state ηR_0 , where R_0 is the bright-state atom's scattering rate, and η is the detection efficiency of the system, the rate at which the scattering rate changes during the probe pulse R_{decay} , and the rate of background counts entering the detector R_{bg} [22]. For each probe frequency, we plot the bright-state error based on $n_{thresh} = 1$ and fit the data to the model. The results are shown in Fig. 3. We measure R_{bg} for each data set using the photons counted for those trials in which an atom is not trapped. We also measure the detection efficiency η of our system using the saturation method detailed in [12]. R_0 and R_{decay} are left as free parameters in the model.

The results of the fitting procedure are given in Tbl. I. The background rate R_{bg} is relatively consistent across all three data sets, so the shape of the curve is dependent on the interplay between R_0 and R_{decay} . Initially, ϵ_B falls quickly at a rate governed by R_0 before leveling off due to the loss in counts caused by R_{decay} . Thus, the lowest

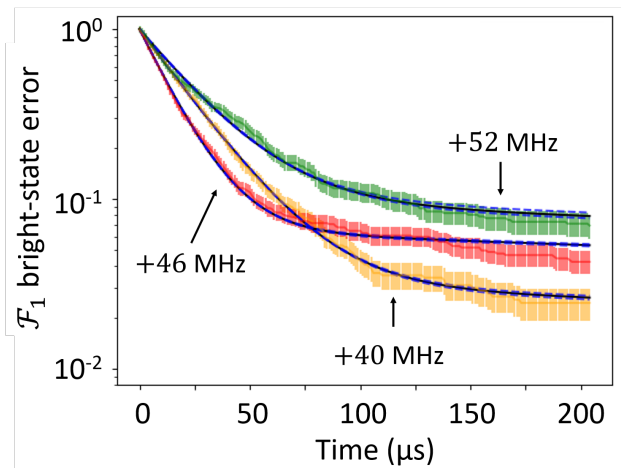


FIG. 3. \mathcal{F}_1 bright-state error rates for three probe frequencies. The solid lines are the fits to the protocol model with the dashed lines representing the 95% confidence levels.

TABLE I. The values for ηR_0 and R_{decay} at each probe frequency extracted from the protocol model fit to experimental data. The measured R_{bg} are included for completeness. The values are given in kilo-counts per second (kcps)

Probe f	R_{bg} (kcps)	ηR_0 (kcps)	R_{decay} (kcps)	$\eta R_0 / R_{decay}$
+40 MHz	1.05	39.4 ± 0.2	1.31 ± 0.04	30.08
+46 MHz	1.13	58.7 ± 0.5	4.1 ± 0.1	14.3
+52 MHz	1.12	33.6 ± 0.3	3.63 ± 0.1	8.2

possible bright-state error is achieved for the largest ratio of R_0 and R_{decay} . This occurs for the +40 MHz readout beam, mainly because R_{decay} is smallest for this case. This is opposite to our intuition about ORP, because this readout-beam frequency is tuned closest to the $F' = 2$ excited state.

We believe that multiple factors are contributing to R_{decay} . One is heating caused by the probe beam during readout. As the atom heats, it samples a larger range of trap depths and is farther detuned from the probe beam, lowering the scattering rate [22]. Heating is known to be important for single-atom traps [9, 21] and may contribute to the increase in R_{decay} on and above resonance, where heating is known to be worse [23].

We look for evidence of heating in our system by comparing the frequency-dependence of the atomic fluorescence during quantum state readout to that seen during atom detection, when cooling is present. The data is plotted in the top panel of Fig. 4. The solid line is a rate equation model of the system that does not include heating. We see that it accurately predicts atomic behavior when the atom remains cold, but fails during quantum state readout. Near and above resonance, we see that the atomic fluorescence is suppressed during the

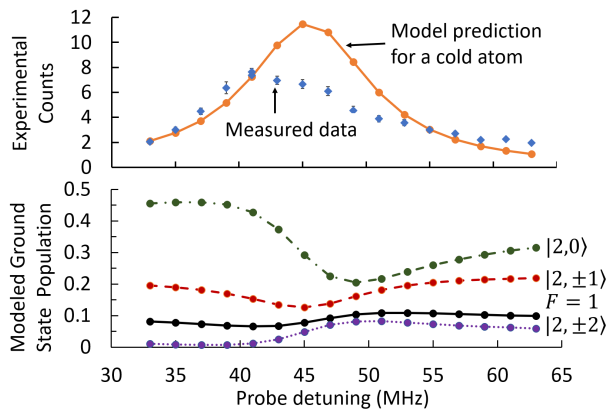


FIG. 4. *Top Panel* Compared to the prediction for a cold atom (orange) the atomic fluorescence (blue) is suppressed at higher detunings. *Bottom Panel* Rate-equation model predictions for the ground state atomic sublevel populations for various probe beams.

quantum state readout. This is the behavior captured by R_{decay} . The peak fluorescence during readout occurs at a detuning near the half-width at half-maximum of the cooled atom’s broadened resonance, the location known to minimize Doppler heating [16]. This supports the hypothesis that heating is a cause of R_{decay} . Time-resolved fluorescence detection of single-atoms, such as that demonstrated here, could be a useful tool for further investigating such heating effects. Incorporating such effects into a rate-equation model of the atom-probe system would be a natural extension of this work.

Heating is likely a significant cause of R_{decay} , but off-resonant pumping is known to contribute as well, and we would still expect it to be worse below peak-resonance. Our rate equation model contains the mechanisms for off-resonant pumping and can shed light on this physical process. The ground state populations predicted by the rate equation model are shown in the bottom panel of Fig. 4. We see that the $F = 1$ population, which is proportional to the amount of ORP, actually peaks above the location of the shifted resonance. This surprising result can be understood by considering the $F = 2$ sublevel populations, also shown in Fig. 4. The atomic population always preferentially accrues in the $m_F = 0$ state due to the Clebsch-Gordan coefficients of the relevant transitions. This state is relatively protected from ORP because the $|2,0\rangle \rightarrow |2,0\rangle$ transition is quantum mechanically forbidden. At frequencies below the $|2,0\rangle \rightarrow |3,0\rangle$ transition, this protected state dominates the population, suppressing transfer of population to $F = 1$. At higher frequencies, however, more atomic population accrues in the $|2,\pm 1\rangle$ and $|2,\pm 2\rangle$ states. These states are not protected from ORP in the same way, so the amount of population in $F = 1$ increases. Thus, we see that the use

of π -polarized light tuned at or below the atomic resonance exploits the quantum mechanical selection rules to suppress ORP.

We have shown that state readout fidelity depends on three parameters: R_{bg} , ηR_0 , and R_{decay} . This is a powerful model for optimizing non-destructive state detection. Decreasing R_{bg} lowers the dark-state error and improves fidelity. The background rate is around 700 cps for the data presented in Fig. 2. The largest source of background scatter in our experiment is stray scatter from the probe beam. This can be decreased by focusing the probe beam, therefore decreasing the power needed to reach the desired intensity [15] and by using a fiber with a smaller collection core to improve spatial filtering. Both of these techniques greatly increase the alignment difficulty of the system and were beyond the scope of this work.

The bright-state error can be reduced by increasing ηR_0 and decreasing R_{decay} . In our system, we measure a total detection efficiency of 0.96% [12]. Aberrations in the imaged fluorescence are the main source of loss in our collection path. Improved alignment, which is not experimentally trivial, should increase the collection efficiency. Using the readout model described here, we estimate that increasing η by a factor of two is feasible and will yield a peak fidelity of $F_2 = 98.8\%$ in a $\sim 75\text{-}\mu\text{s}$ -long detection time. Clearly, linearly-polarized readout light offers a promising route to fast, nondestructive quantum-state readout.

The final parameter of interest, R_{decay} is less straightforward to change, as it likely depends on both ORP and heating of the atom. A demonstrated method to suppress ORP is to prepare the atom into the one of the $m_F = \pm 2$ states and use circularly polarized readout light on the $|2,2\rangle \rightarrow |3,3\rangle$ cycling transition. This has been shown to achieve readout fidelities of $> 98\%$ [15–17] but requires a more complicated state preparation scheme than that used here. Furthermore, pumping the atom into the stretched state is relatively slow because of the differential shifts caused by the ODT [12]. Linearly-polarized readout schemes like that presented here and in [18] are consistently an order of magnitude faster than those utilizing circularly-polarized light [15–17].

In conclusion, we demonstrate the fastest non-destructive quantum-state readout yet reported for neutral atoms. Using linearly-polarized light and time-tagging the detected photons, we investigate the time-dependence of the atomic scattering rate during the probe pulse and identify a surprising protection from ORP by tuning the readout light frequency to just below resonance. These techniques can be used to further understand the interaction of single, neutral atoms with near-resonant laser light and off-resonant trapping light.

We gratefully acknowledge the support of the US Army Research Office cooperative agreement Award No. W911NF-15-2-0047.

-
- [1] M. Saffman, *Journal of Physics B: Atomic, Molecular and Optical Physics* **49**, 202001 (2016).
- [2] H. Bernien, S. Schwartz, A. Keesling, H. Levine, A. Omran, H. Pichler, S. Choi, A. S. Zibrov, M. Endres, M. Greiner, V. Vuletić, and M. D. Lukin, *Nature* **551**, 579 EP (2017), article.
- [3] H. Labuhn, D. Barredo, S. Ravets, S. de Léséleuc, T. Macrì, T. Lahaye, and A. Browaeys, *Nature* **534**, 667 EP (2016).
- [4] H. Levine, A. Keesling, G. Semeghini, A. Omran, T. T. Wang, S. Ebadi, H. Bernien, M. Greiner, V. Vuletić, H. Pichler, and M. D. Lukin, *Phys. Rev. Lett.* **123**, 170503 (2019).
- [5] I. S. Madjarov, J. P. Covey, A. L. Shaw, J. Choi, A. Kale, A. Cooper, H. Pichler, V. Schkolnik, J. R. Williams, and M. Endres, *Nature Physics* (2020), 10.1038/s41567-020-0903-z.
- [6] T. M. Graham, M. Kwon, B. Grinkemeyer, Z. Marra, X. Jiang, M. T. Lichtman, Y. Sun, M. Ebert, and M. Saffman, *Phys. Rev. Lett.* **123**, 230501 (2019).
- [7] H. Levine, A. Keesling, A. Omran, H. Bernien, S. Schwartz, A. S. Zibrov, M. Endres, M. Greiner, V. Vuletić, and M. D. Lukin, *Phys. Rev. Lett.* **121**, 123603 (2018).
- [8] R. Bourgain, J. Pellegrino, S. Jennewein, Y. R. P. Sortais, and A. Browaeys, *Opt. Lett.* **38**, 1963 (2013).
- [9] Y.-S. Chin, M. Steiner, and C. Kurtsiefer, *Phys. Rev. A* **95**, 043809 (2017).
- [10] R. Noek, G. Vrijsen, D. Gaultney, E. Mount, T. Kim, P. Maunz, and J. Kim, *Opt. Lett.* **38**, 4735 (2013).
- [11] S. Crain, C. Cahall, G. Vrijsen, E. E. Wollman, M. D. Shaw, V. B. Verma, S. W. Nam, and J. Kim, *Communications Physics* **2**, 97 (2019).
- [12] M. E. Shea, J. Kim, and D. J. Gauthier, In preparation (2018).
- [13] D. J. Wineland, J. C. Bergquist, W. M. Itano, and R. E. Drullinger, *Opt. Lett.* **5**, 245 (1980).
- [14] A. H. Myerson, D. J. Szwer, S. C. Webster, D. T. C. Allcock, M. J. Curtis, G. Imreh, J. A. Sherman, D. N. Stacey, A. M. Steane, and D. M. Lucas, *Phys. Rev. Lett.* **100**, 200502 (2008).
- [15] A. Fuhrmanek, R. Bourgain, Y. R. P. Sortais, and A. Browaeys, *Phys. Rev. Lett.* **106**, 133003 (2011).
- [16] M. Kwon, M. F. Ebert, T. G. Walker, and M. Saffman, *Phys. Rev. Lett.* **119**, 180504 (2017).
- [17] M. Martinez-Dorantes, W. Alt, J. Gallego, S. Ghosh, L. Ratschbacher, Y. Völzke, and D. Meschede, *Phys. Rev. Lett.* **119**, 180503 (2017).
- [18] M. J. Gibbons, C. D. Hamley, C.-Y. Shih, and M. S. Chapman, *Phys. Rev. Lett.* **106**, 133002 (2011).
- [19] C.-Y. Shih and M. S. Chapman, *Phys. Rev. A* **87**, 063408 (2013).
- [20] M. E. Shea and D. J. Gauthier, *Phys. Rev. A* **96**, 027401 (2017).
- [21] M. Martinez-Dorantes, W. Alt, J. Gallego, S. Ghosh, L. Ratschbacher, and D. Meschede, *Phys. Rev. A* **97**, 023410 (2018).
- [22] M. E. Shea, *Fast, Nondestructive, Quantum-state Read-out of a Single, Trapped, Neutral Atom*, Ph.D. thesis, Duke University (2018).
- [23] H. Metcalf and P. van der Straten, *Laser Cooling and Trapping*, Graduate Texts in Contemporary Physics (Springer New York, 2001).